Published in final edited form as:
Curr Biol. 2008 September 9; 18(17): 1333–1337. doi:10.1016/j.cub.2008.07.086.

The *C. elegans* Zonula Occludens Ortholog ZOO-1 Cooperates with the Cadherin-Catenin Complex to Recruit Actin during Epidermal Morphogenesis

Christina Lockwood[1,3], **Ronen Zaidel-Bar**[2], and **Jeff Hardin**[1,2,*]

1*Program in Cellular and Molecular Biology, University of Wisconsin-Madison, 1117 W. Johnson Street, Madison, WI 53706*

2*Department of Zoology, University of Wisconsin-Madison, 1117 W. Johnson Street, Madison, WI 53706*

Summary

The dramatic cell shape changes necessary to form a multicellular organism require cell-cell junctions to be both pliable and strong. The Zonula Occludens (ZO) subfamily of membrane-associated guanylate kinases (MAGUKs) are scaffolding molecules thought to regulate cell-cell adhesion [1–3], but there is little known about their roles in vivo. To elucidate the functional role of ZO proteins in a living embryo, we have characterized the sole *C. elegans* ZO family member, ZOO-1. ZOO-1 localizes with the cadherin-catenin complex during development and its junctional recruitment requires the transmembrane proteins HMR- 1/E-cadherin and VAB-9/claudin, but surprisingly, not HMP-1/α-catenin or HMP-2/β-catenin. *zoo-1* knockdown results in lethality during elongation, resulting in the rupture of epidermal cell-cell junctions under stress and failure of epidermal sheet sealing at the ventral midline. Consistent with a role in recruiting actin to the junction in parallel to the cadherin-catenin complex, *zoo-1* loss of function reduces the dynamic recruitment of actin to junctions and enhances the severity of actin filament defects in hypomorphic alleles of *hmp-1* and *hmp-2*. These results show that ZOO-1 cooperates with the cadherin-catenin complex to dynamically regulate strong junctional anchorage to the actin cytoskeleton during morphogenesis.

Results and Discussion

ZOO-1, the sole Zonula Occludens Ortholog in *C. elegans*, localizes to junctions during morphogenesis

The *C. elegans* genome contains a single predicted ortholog of the Zonula Occludens protein family, ORF Y105E8A.26, which we have named *zoo-1*, for Zonula Occludens ortholog (Supplemental Figure 1). We assayed ZOO-1 expression via immunostaining (Figure 1; Supplemental Figure 2); a *zoo-1::gfp* construct shows identical localization (Movie 1). During morphogenesis, ZOO-1 becomes enriched at the borders of epidermal cells (Figure 1A; Supplemental Figure 2D–F); elongating embryos exhibit the strongest junctional accumulation (Supplemental Figure 2G, H). ZOO-1 is also expressed in myoblasts and persists in mature

*Corresponding Author, Jeff Hardin, Department of Zoology, University of Wisconsin-Madison, 1117 W. Johnson Street, Madison, WI 53706, Tel: 608-262-9634, Fax: 608-262-7319, Email: jdhardin@wisc.edu.
[3]Present address: Washington University School of Medicine, Department of Pathology & Immunology, 660 S Euclid, Campus Box 8118, St. Louis, MO 63110

muscle cells (Supplemental Figure 2G). In contrast, *zoo-1::gfp* driven using an epithelial promoter shows no muscle-associated signal (data not shown); thus muscle-associated ZOO-1 signal is due to expression specifically in muscle.

In cultured epithelial cells, ZO-1 initially associates with the adherens junction (AJ) and segregates apically to the tight junction as cells mature [4–7]. The apical junction in epidermal cells of *C. elegans* has two subdomains with distinct multiprotein complexes, the cadherin-catenin and DLG-AJM complexes [8], which can be partially resolved using light microscopy in embryos [9]. Quantitative colocalization analysis shows a high degree of overlap between ZOO- 1, HMP-1/α-catenin and JAC-1/p120 catenin but not between ZOO-1 and the DLG-1/AJM-1 complex (Supplemental Figure 3).

ZOO-1 recruitment to junctions is HMR-1/cadherin and VAB-9/BCMP1 dependent but HMP-1/α-catenin and HMP-2/β-catenin independent

We next examined molecular requirements for ZOO-1 recruitment. Unlike AJM-1, which depends on DLG-1/Discs large for localization, ZOO-1 localizes properly in *dlg-1(RNAi)* embryos (Figure 1D–F). Previous work in tissue culture has suggested that localization of vertebrate ZO-1 to the AJ may depend on α-catenin [10, 11]. We tested this *in vivo* by immunostaining *hmp-1(zu278)* null embryos for ZOO-1. However, ZOO-1 junctional localization appears largely unaffected in *hmp-1* zygotic null embryos (data not shown), as it does in *hmp-1(RNAi)* (Figure 1G–I) or *hmp-2/β-catenin (RNAi)* embryos (data not shown), in which both maternal and zygotic mRNA are removed [12, 13]. In contrast, *hmr-1/E-cadherin (RNAi)* completely disrupts epidermal ZOO-1 localization (Figure 1J–L), although localization in muscle is unaffected. VAB-9/BCMP1 also localizes to the cadherin-catenin complex in epidermal cells in *C. elegans* [9]; ZOO-1 expression in *vab-9(ju6)* mutants is very similar to that in *hmr-1(RNAi)* embryos (Figure 1M–O). These results suggest that both HMR-1 and VAB-9 are essential for recruiting ZOO-1 to the apical junction, but that they act upstream of HMP-2 and HMP-1.

Vertebrate ZO proteins directly interact with multiple claudin family members [14,15]. However, we could detect no effects on junctional recruitment of ZOO-1 in *clc-1/2* single or double RNAi embryos nor epithelial permeability defects in *zoo-1* loss of function embryos in a standard assay [16] (data not shown). These data suggest that ZOO-1 is not an essential component of the paracellular permeability pathway in *C. elegans*.

zoo-1 knockdown results in morphogenesis defects

To examine consequences of loss of *zoo-1* function, we analyzed two *zoo-1* mutants, but both result in incomplete loss of *zoo-1* gene function (Supplementary Results). In order to achieve more complete *zoo-1* loss of function, we performed RNAi in an RNAi hypersensitive background (*rrf-3(pk1426)*; [17]). *zoo-1(RNAi);rrf-3* embryos have no detectable ZOO-1 expression as assessed via immunostaining (Supplemental Figure 4), and knockdown can be achieved using multiple different RNAs that target *zoo-1* (data not shown). *rrf-3(pk1426)* homozygotes exhibit low levels of embryonic lethality (11.4 ± 6.3%, mean ± SD, n=272) prior to the initiation of epidermal morphogenesis, due to gastrulation failure (data not shown). Although the penetrance of gastrulation defects in double mutants is similar to *rrf-3* single mutants, *zoo-1(RNAi)* in an *rrf-3(pk1426)* background increased overall lethality to 33.2 ± 5.9% (n=247) and yielded multiple morphogenetic defects (Figure 2). *zoo-1(RNAi);rrf-3* embryos (Figure 2G–I) properly complete ventral enclosure and initiate elongation; however, the rate of elongation is markedly slower than in wild-type (Figure 2A–C and Movie 2) or *rrf-3* animals (Figure 2D–F and Movie 3), and abnormal bulges develop along the body (Figure 2I). Body wall muscle is functional in arrested *zoo-1;rrf-3* embryos, which continue to twitch, and muscle morphology appears normal via phalloidin staining (Supplemental Figure 4H),

suggesting these defects are epidermal in nature. 6% of *zoo-1(RNAi);rrf-3* embryos exhibit epidermal rupture during elongation (Figure 2J–L and Movie 4). The distribution and dynamics of HMP-1::GFP and JAC-1::GFP are normal in living *zoo-1(RNAi);rrf-3* embryos, and we could not detect enhancement of morphogenetic defects following ZOO-1 depletion in *vab-9 (ju6)* null mutants (data not shown). The simplest interpretation of these results is that ZOO-1 acts downstream of VAB-9 to stabilize junctional integrity.

That *zoo-1(RNAi);rrf-3* embryos rupture suggests reduced resistance of apical junctions to actomyosin-mediated contractility. We therefore generated hypocontractile *zoo-1 (RNAi);rrf-3* embryos using simultaneous weak RNAi against *let-502*/Rho kinase, and we enhanced contractility by performing *zoo-1(RNAi)* in *mel-11(it26)*/myosin phosphatase mutants, in which myosin presumably remains phosphorylated and hence abnormally active [18]. *let-502(RNAi)* resulted in a reduction of rupture of *zoo-1(RNAi);rrf-3* embryos from 12 to 4% (n = 66 and 116 embryos examined, respectively; significantly different, $p < 0.04$, Fisher's exact test), whereas *zoo-1(RNAi)* knockdown in *mel-1(it26)* homozygotes resulted in the appearance of early ruptures prior to the 1.5-fold stage (n = 53 and 22 embryos examined for *zoo-1(RNAi);mel-11(it26)* and *mel-11(it26)*, respectively; Figure 2M–O, Supplemental Figure 5; significantly different from *mel-11* alone, $p < 0.008$). Based on these results, we conclude that ZOO-1 is especially important to provide mechanical stability to epidermal junctions.

zoo-1 (RNAi) reduces junctional actin recruitment, leading to perturbed actin filaments

We next visualized actin dynamics with an F-actin reporter expressed specifically in the epidermis, the actin-binding domain of VAB-10 fused to GFP [19]. We observed a significant decrease in actin localized near cell-cell junctions. Actin in this region aligns into a robust cable parallel to cell-cell boundaries in *rrf-3* embryos (Figure 3A,C), whereas in *zoo-1 (RNAi);rrf-3* embryos junctional actin is less robust (Figure 3B,D). Quantitative analysis (see Supplemental Figure 6 for description) confirms these observations: the ratio of junctional to cytoplasmic actin in wildtype is 2.16 ± 0.26 (mean ± SD, n = 22 cells in 4 embryos measured) vs. 1.4 ± 0.2 in *zoo- 1(RNAi);rrf-3* embryos (n = 23 cells in 5 embryos; significantly different based on a two-tailed student t-test, $p < 0.01$). During elongation, actomyosin contractile forces act along circumferential actin bundles (CFBs), which attach at their ends to cell-cell junctions and are thought to distribute the forces driving elongation. In untreated embryos CFBs are evenly spaced (Figure 3E). Strikingly, in *zoo-1 (RNAi)* embryos some CFBs cluster abnormally (Figure 3F), suggesting that ZOO-1 contributes to their anchorage.

Since some *zoo-1(RNAi);rrf-3* embryos rupture during elongation, we imaged F-actin during ventral enclosure, when midline junctional connections are established. In contrast to wild-type embryos, which accumulate robust junctional actin at the ventral midline (Figure 3A; Movie 5), in *zoo-1(RNAi);rrf-3* embryos that display midline bulges near the end of enclosure we consistently found loss of accumulation of midline junctional actin (Figure 3B; n = 6/6 embryos with midline defects examined), or failure to establish a midline connection entirely between one or more cells (Movie 6 and Movie 7; n = 4/6 embryos with midline junctional failure). Taken together, the abnormalities in actin organization we observe in *zoo-1* knockdown embryos provide a mechanical explanation for observed defects at the end of ventral enclosure and during elongation.

zoo-1 (RNAi) enhances the lethality of *hmp-1*/α-catenin and *hmp-2*/β-catenin hypomorphs

Connecting the actin cytoskeleton to cell-cell junctions is a role traditionally assigned to the cadherin-catenin complex [20]. Since ZOO-1 recruitment is independent of both α- and β-catenin, we hypothesized that ZOO-1 recruits actin to the junction in a parallel pathway. To test this hypothesis we examined the combined effects of *zoo-1* (RNAi) and weak loss of

function for β-catenin and α-catenin, using *hmp-2* (*qm39*) ([21]; M. Costa, pers. comm.) and *hmp-1(fe4)* [22], respectively. *hmp-2(qm39)* displays 6 ± 1.2% (n=832) embryonic and early larval lethality at 20°C (Table 1). In *hmp-2(qm39);zoo-1(RNAi)* embryos, lethality is significantly enhanced to 60 ± 4.6% (n=508) and mutants exhibit delayed development (Table 1). Unlike wild-type embryos (Figure 4A), progeny of *hmp-1(fe4)* hermaphrodites show pronounced elongation defects (Figure 4B and Movie 8), and exhibit 77.5 ± 7.9% (n=844) embryonic and early larval lethality (Table 1; [22]). Phalloidin staining of *hmp-1(fe4)* embryos confirms that the spatial arrangement of CFBs is occasionally perturbed ([27]; Figure 4E). *zoo-1(RNAi)* in *hmp-1(fe4)* mutants enhances overall lethality to 99.6 ± 1.8% (n=818), and causes nearly all embryos to exhibit the Humpback phenotype (Figure 4D and Movie 9). Approximately half of *zoo-(RNAi);hmp-1(fe4)* mutants ultimately rupture at various positions along the body axis (Figure 4C and Movie 10).

zoo-1 loss of function also exacerbates the cytoskeletal defects observed in *hmp-1(fe4)* embryos: CFBs often cluster, resulting in inappropriately thick bundles (Figure 4F) similar to *hmp-1* null mutants and the most severe *hmp-1(fe4)* embryos [12, 22], suggesting that ZOO-1 and the cadherin complex actin in parallel to stabilize actin at epidermal junctions. Loss of UNC- 34/Ena also synergizes with *hmp-1(fe4)*, but unlike ZOO-1, UNC-34 is correctly localized in *hmr-1* mutant backgrounds [23]. We found no evidence for synergistic lethality between *zoo-1* and the null allele, *unc-34(gm104)* (data not shown).

In conclusion, we have provided the first *in vivo* analysis of ZOO-1/ZO-1 in *C. elegans*, and show that ZOO-1 acts at junctions along with core AJ proteins during epithelial morphogenesis. Recent studies in *Drosophila* have implicated ZO-1/Pyd at AJs, based on defects in cell rearrangement during tracheal morphogenesis in *pyd* mutants [24]. However, these same studies have also implicated *pyd* in nuclear functions. Because it lacks the nuclear localization sequence found in other ZO-1 orthologues, ZOO-1 provides a "natural experiment" that can identify exclusively non-nuclear roles for ZO-1 proteins.

In ZO-1/ZO-2/ZO-3 knockdown cells in culture, AJ maturation is delayed [25]. In contrast, we do not find a delay in recruitment of core AJ components in *zoo-1* knockdown embryos in vivo. It is possible that the extremely rapid kinetics of junction formation in model invertebrates (minutes, as opposed to many hours in vertebrates) accounts for this difference, as has been previously suggested [22]. However, dynamic imaging of actin in living embryos following *zoo-1* knockdown revealed dramatic effects on actin recruitment at maturing junctions, which may be analogous to defects observed in the transition from "spot-like" to "belt-like" AJs in cultured cells following ZO protein depletion [25,26]. Although ZO-1 directly binds actin [11,27], the lack of sequence conservation in this region of ZOO-1 does not immediately suggest that ZOO-1 does so. Unfortunately, the dominant lethality of *zoo-1* transgenes has thus far precluded unambiguous structure-function analysis to address this issue.

C. elegans embryos undergoing epidermal morphogenesis do not require HMP-1/α- catenin or HMP-2/β-catenin for junctional recruitment of ZOO-1. In contrast, ZOO-1 recruitment does depend on HMR-1/E-cadherin and VAB-9/BCMP1. Since HMR-1 is required for proper junctional localization of VAB-9 [9], the simplest explanation for these localization results is HMR-1→VAB-9→→ZOO-1. Since there are very few cytoplasmic residues in VAB-9 that could engage in direct binding to ZOO-1, we think it unlikely that the interaction between the two proteins is direct. Instead, another protein presumably recruits ZOO-1 to AJs. Future studies that characterize the binding affinities of ZOO-1 at epidermal junctions should clarify the role of this highly conserved protein during morphogenesis.

Supplementary Material

Refer to Web version on PubMed Central for supplementary material.

Acknowledgements

We thank members of the Hardin lab for helpful discussion, Chris Lockwood for sharing unpublished data on *mel-11 (it26)*, and M. Costa for sharing unpublished results regarding *hmp-2(qm39)*. Reagents were generously provided by Y. Kohara (cDNAs), L. Segalat (strain containing *zoo-1(cxTi8317))*, the International *C. elegans* Knockout Consortium (strain containing *zoo-1(gk404)*), and M. Labouesse (strain containing *vab-10::ABD::gfp*). Some *C. elegans* strains were obtained from the *C. elegans* Genetics Stock Center, which is funded by a grant from the NIH National Center for Research Support. This work was supported by NIH grant GM058038 to JH. RZB was supported by NIH postdoctoral training grant GM078747 and by a grant from the Machaiah Foundation.

REFERENCES

1. Funke L, Dakoji S, Bredt DS. Membrane-associated guanylate kinases regulate adhesion and plasticity at cell junctions. Annu Rev Biochem 2005;74:219–245. [PubMed: 15952887]
2. Shin K, Fogg VC, Margolis B. Tight junctions and cell polarity. Annu Rev Cell Dev Biol 2006;22:207–235. [PubMed: 16771626]
3. Yap AS, Crampton MS, Hardin J. Making and breaking contacts: the cellular biology of cadherin regulation. Curr Opin Cell Biol 2007;19:508–514. [PubMed: 17935963]
4. Fesenko I, Kurth T, Sheth B, Fleming TP, Citi S, Hausen P. Tight junction biogenesis in the early Xenopus embryo. Mech Dev 2000;96:51–65. [PubMed: 10940624]
5. Rajasekaran AK, Hojo M, Huima T, Rodriguez-Boulan E. Catenins and zonula occludens-1 form a complex during early stages in the assembly of tight junctions. J Cell Biol 1996;132:451–463. [PubMed: 8636221]
6. Sheth B, Fontaine JJ, Ponza E, McCallum A, Page A, Citi S, Louvard D, Zahraoui A, Fleming TP. Differentiation of the epithelial apical junctional complex during mouse preimplantation development: a role for rab13 in the early maturation of the tight junction. Mech Dev 2000;97:93–104. [PubMed: 11025210]
7. Yonemura S, Itoh M, Nagafuchi A, Tsukita S. Cell-to-cell adherens junction formation and actin filament organization: similarities and differences between non-polarized fibroblasts and polarized epithelial cells. J Cell Sci 1995;108(Pt 1):127–142. [PubMed: 7738090]
8. Cox EA, Hardin J. Sticky worms: adhesion complexes in C. elegans. J Cell Sci 2004;117:1885–1897. [PubMed: 15090594]
9. Simske JS, Koppen M, Sims P, Hodgkin J, Yonkof A, Hardin J. The cell junction protein VAB-9 regulates adhesion and epidermal morphology in C. elegans. Nat Cell Biol 2003;5:619–625. [PubMed: 12819787]
10. Imamura Y, Itoh M, Maeno Y, Tsukita S, Nagafuchi A. Functional domains of alpha-catenin required for the strong state of cadherin-based cell adhesion. J Cell Biol 1999;144:1311–1322. [PubMed: 10087272]
11. Itoh M, Nagafuchi A, Moroi S, Tsukita S. Involvement of ZO-1 in cadherin-based cell adhesion through its direct binding to alpha catenin and actin filaments. J Cell Biol 1997;138:181–192. [PubMed: 9214391]
12. Costa M, Raich W, Agbunag C, Leung B, Hardin J, Priess JR. A putative catenin-cadherin system mediates morphogenesis of the Caenorhabditis elegans embryo. J Cell Biol 1998;141:297–308. [PubMed: 9531567]
13. Raich WB, Agbunag C, Hardin J. Rapid epithelial-sheet sealing in the Caenorhabditis elegans embryo requires cadherin-dependent filopodial priming. Curr Biol 1999;9:1139–1146. [PubMed: 10531027]
14. Schneeberger EE, Lynch RD. The tight junction: a multifunctional complex. Am J Physiol Cell Physiol 2004;286:C1213–C1228. [PubMed: 15151915]
15. Miyoshi J, Takai Y. Molecular perspective on tight-junction assembly and epithelial polarity. Adv Drug Deliv Rev 2005;57:815–855. [PubMed: 15820555]

16. Asano A, Asano K, Sasaki H, Furuse M, Tsukita S. Claudins in Caenorhabditis elegans: their distribution and barrier function in the epithelium. Curr Biol 2003;13:1042–1046. [PubMed: 12814550]

17. Simmer F, Tijsterman M, Parrish S, Koushika SP, Nonet ML, Fire A, Ahringer J, Plasterk RH. Loss of the putative RNA-directed RNA polymerase RRF-3 makes C. elegans hypersensitive to RNAi. Curr Biol 2002;12:1317–1319. [PubMed: 12176360]

18. Wissmann A, Ingles J, McGhee JD, Mains PE. Caenorhabditis elegans LET-502 is related to Rho-binding kinases and human myotonic dystrophy kinase and interacts genetically with a homolog of the regulatory subunit of smooth muscle myosin phosphatase to affect cell shape. Genes Dev 1997;11:409–422. [PubMed: 9042856]

19. Liegeois S, Benedetto A, Michaux G, Belliard G, Labouesse M. Genes required for osmoregulation and apical secretion in Caenorhabditis elegans. Genetics 2007;175:709–724. [PubMed: 17179093]

20. Weis WI, Nelson WJ. Re-solving the cadherin-catenin-actin conundrum. J Biol Chem 2006;281:35593–35597. [PubMed: 17005550]

21. Hekimi S, Boutis P, Lakowski B. Viable maternal-effect mutations that affect the development of the nematode Caenorhabditis elegans. Genetics 1995;141:1351–1364. [PubMed: 8601479]

22. Pettitt J, Cox EA, Broadbent ID, Flett A, Hardin J. The Caenorhabditis elegans p120 catenin homologue, JAC-1, modulates cadherin-catenin function during epidermal morphogenesis. J Cell Biol 2003;162:15–22. [PubMed: 12847081]

23. Sheffield M, Loveless T, Hardin J, Pettitt J. C. elegans Enabled exhibits novel interactions with N-WASP, Abl, and cell-cell junctions. Curr Biol 2007;17:1791–1796. [PubMed: 17935994]

24. Jung AC, Ribeiro C, Michaut L, Certa U, Affolter M. Polychaetoid/ZO-1 is required for cell specification and rearrangement during Drosophila tracheal morphogenesis. Curr Biol 2006;16:1224–1231. [PubMed: 16782014]

25. Ikenouchi J, Umeda K, Tsukita S, Furuse M, Tsukita S. Requirement of ZO-1 for the formation of belt-like adherens junctions during epithelial cell polarization. J Cell Biol 2007;176:779–786. [PubMed: 17353356]

26. Yamazaki Y, Umeda K, Wada M, Nada S, Okada M, Tsukita S. ZO-1/2-dependent integration of myosin-2 to epithelial zonula adherens. Mol Biol Cell. 2008

27. Fanning AS, Ma TY, Anderson JM. Isolation and functional characterization of the actin binding region in the tight junction protein ZO-1. Faseb J 2002;16:1835–1837. [PubMed: 12354695]

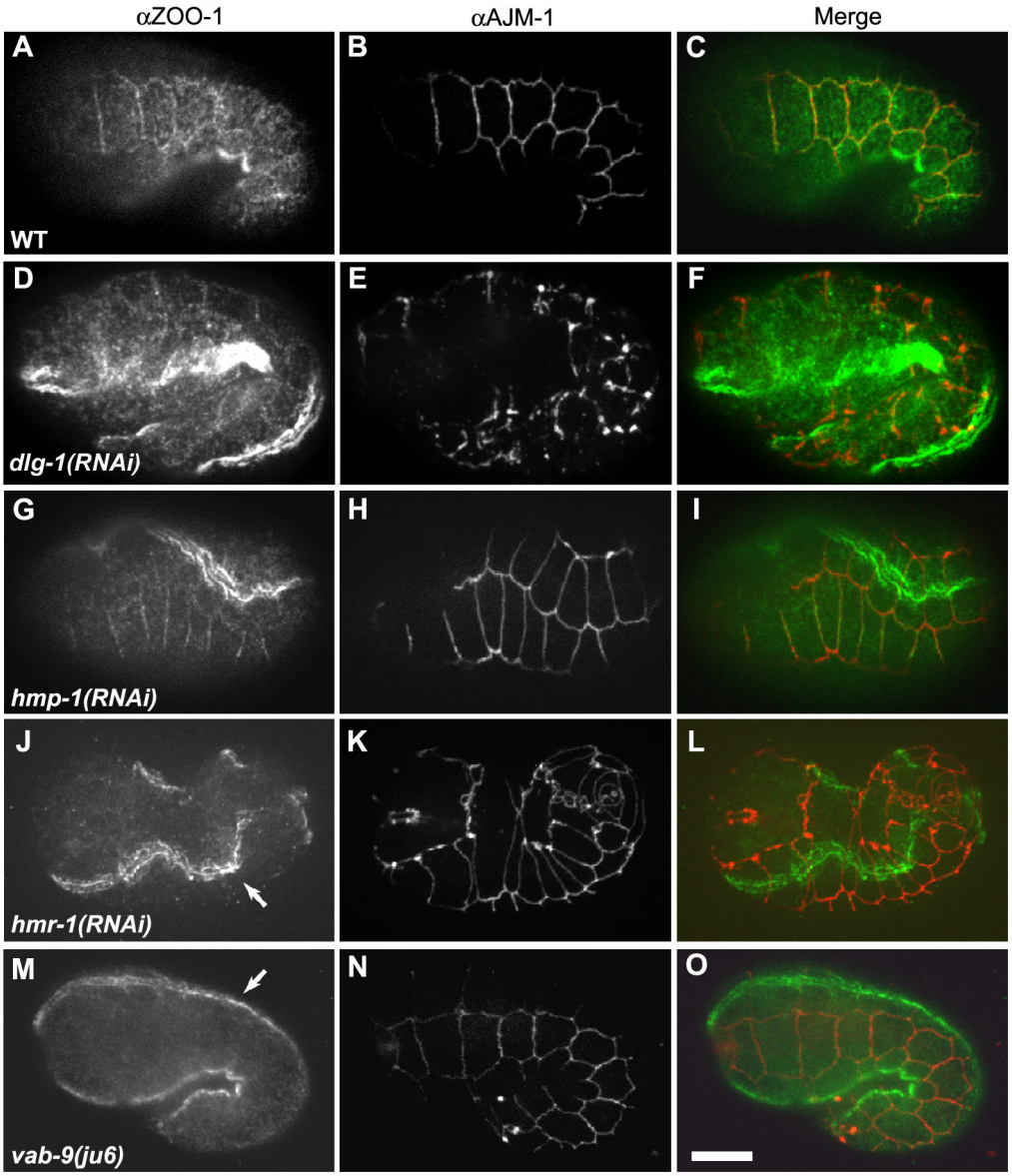

Figure 1. ZOO-1 junctional recruitment is dependent on HMR-1/E-cadherin and VAB- 9/Claudin, but not on HMP-2/β-catenin or HMP-1/α-catenin

(A–L) Confocal images of elongating embryos stained for ZOO-1 (A, D, G, J, M, green), AJM-1 as a junctional marker (B, E, H, K, N, red), and the merged image (C, F, I, L, O). Wild-type (A–C), *dlg-1(RNAi)* (D–F), and *hmp-1(RNAi)* (G–I) embryos display proper junctional localization of ZOO-1, despite disruption of AJM-1 localization in the case of dlg-1(RNAi) (E). (J–L) *hmr-1(RNAi)* embryo exhibits abrogated junctional ZOO-1 staining, though staining persists in sarcomeres (J, arrow). (M–O) *vab-9(ju6)* embryo lacks junctional ZOO-1 staining, though ZOO-1 localization in sarcomeres in unaffected (M, arrow). Scale bar, 10 μm.

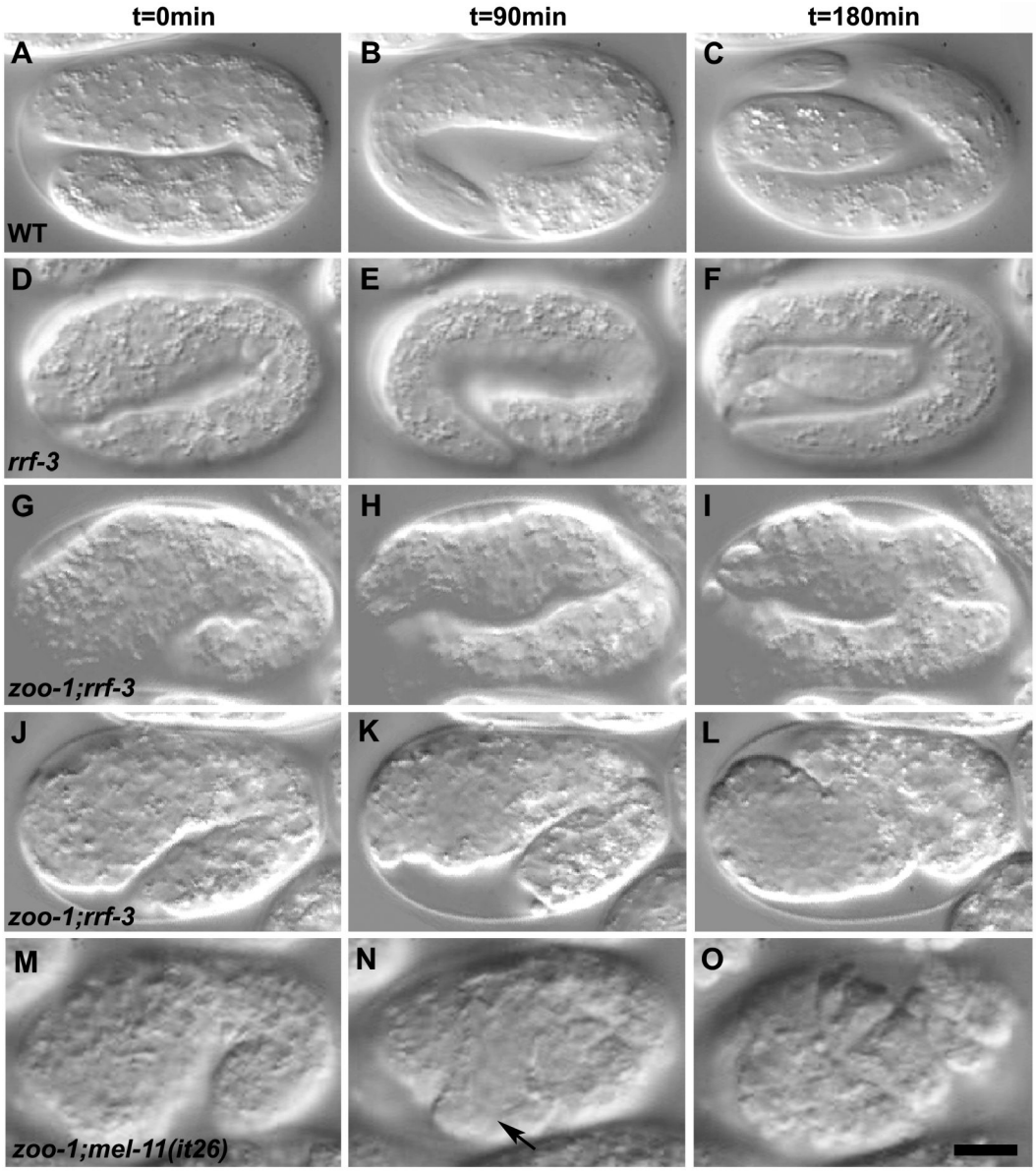

Figure 2. Loss of *zoo-1* function causes embryonic lethality

Nomarski images of representative embryos undergoing elongation are shown. t = 0 correlates with 90 minutes post ventral enclosure. (A–C) Wild-type embryo. (D–F) *rrf-3(pk1426)* embryo. (G–I) *zoo-1(RNAi);rrf-3(pk1426)* embryo exhibiting failed elongation with pronounced body shape defects. (J–L) *zoo-1(RNAi);rrf-3(pk1426)* embryo that has ruptured from the posterior region. Note the delayed elongation of the *zoo-1(RNAi);rrf-3(pk1426)* embryos relative to wildtype. (M–O). *zoo-1(RNAi);mel-11(it26)* embryo. Note the ventral rupture (N, arrow). Scale bar, 10 μm.

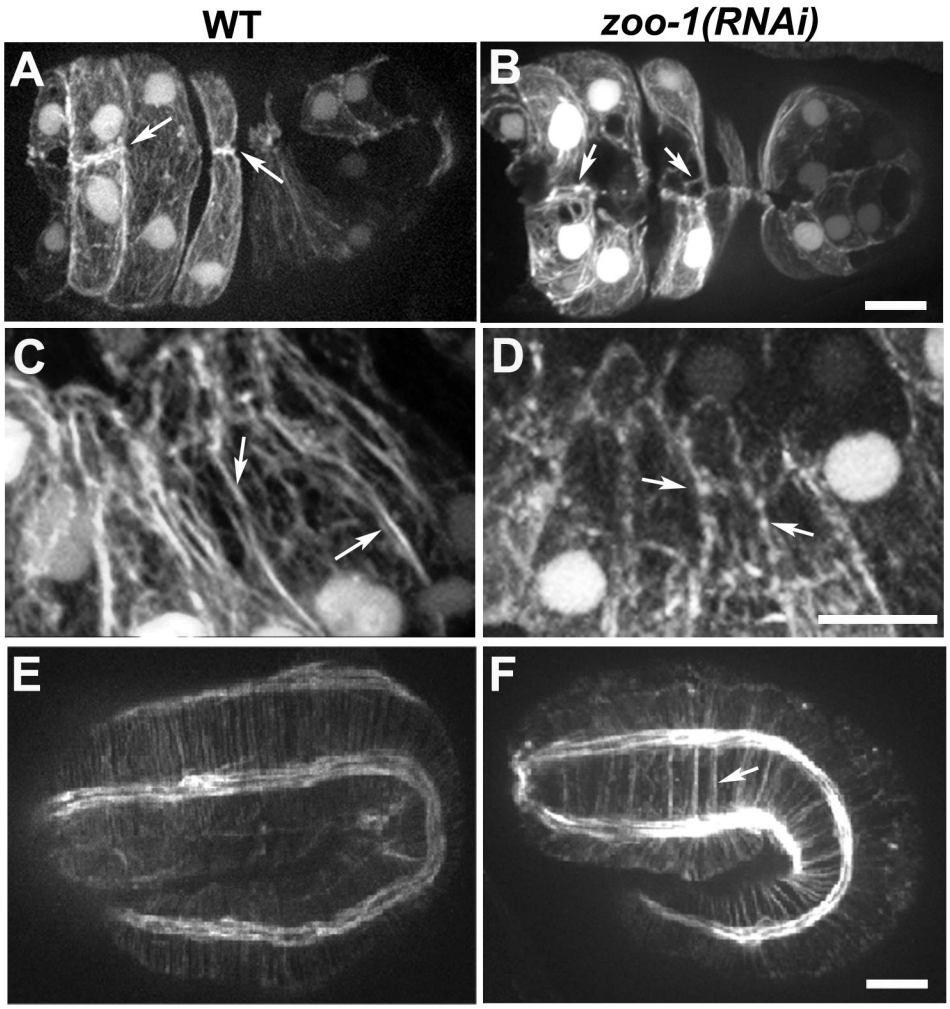

Figure 3. Loss of *zoo-1* function disrupts actin accumulation at cell-cell junctions

(A,B) Ventral views of a wild-type (A) and *zoo-1(RNAi);rrf-3* (B) embryo at the end of ventral enclosure expressing a *gfp*-tagged fragment of *vab-10* that binds F-actin in epidermal cells [41]. In the wild-type embryo, two pairs of anterior cells have accumulated dense actin at the midline (A, arrows), whereas only small actin puncta (B, left arrow) or detached actin filaments (B, right arrow) remain at the same position in the *zoo-1(RNAi);rrf-3* embryo (B, arrows). (C) Robust actin cables are visible at cell-cell borders in epidermal cells in a comma stage embryo (arrows). (D) Actin is less evenly distributed at junctions in epidermal cells of comma stage *zoo-1* knockdown embryos (arrows). (E,F) Embryos at the two-fold stage of elongation stained for F-actin. (E) Wild-type embryo. (F) *zoo-1(RNAi)* embryo. Note the abnormal clustering of circumferential actin filament bundles in the *zoo-1(RNAi)* embryo (arrow). Scale bars, 5 μm.

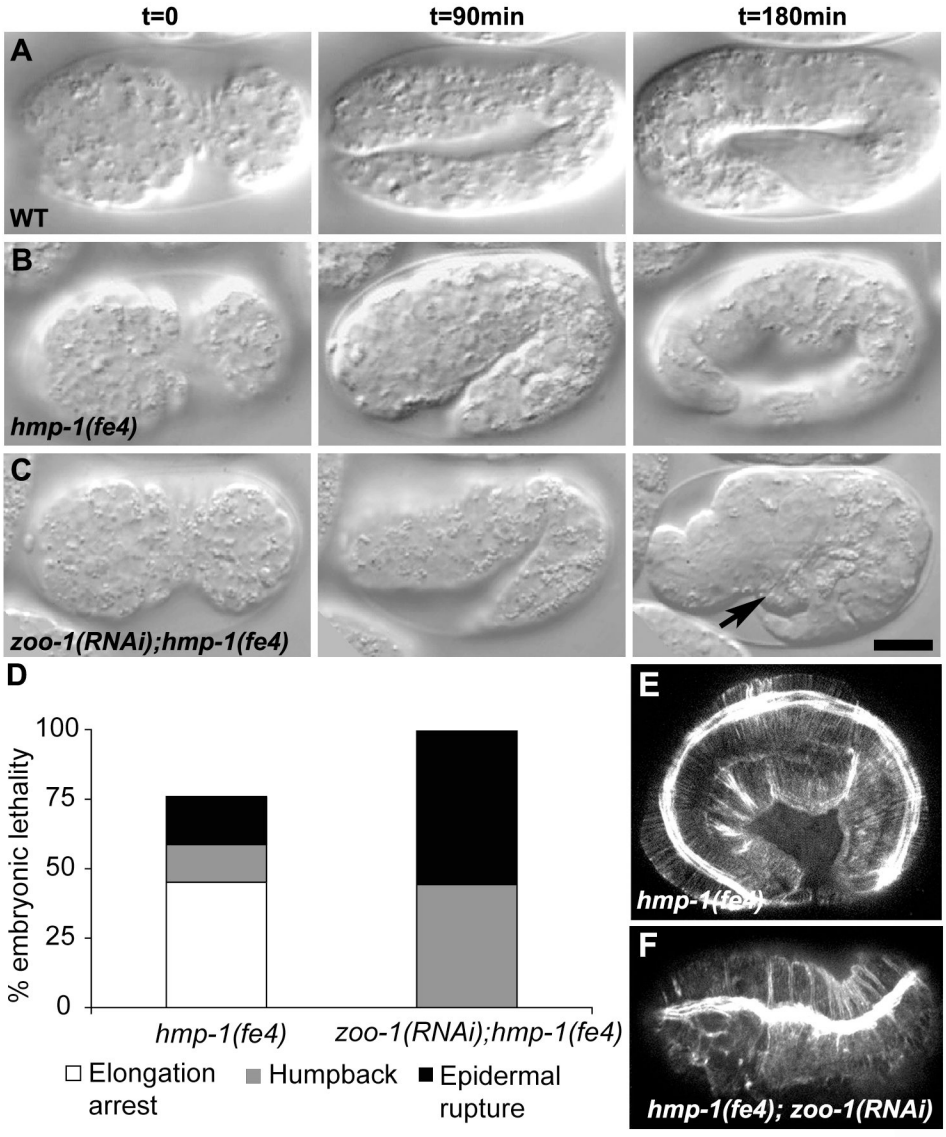

Figure 4. ***zoo-1(RNAi)*** **enhances the elongation defects of** ***hmp-1(fe4)*** **mutants**

(A–C) Nomarski images at 90-minute time intervals of representative embryos undergoing elongation. (B) Wild-type embryo. (B) *hmp-1(fe4)* embryo with visible body shape defects. (C) *zoo-1(RNAi);hmp-1(fe4)* embryo that has ruptured from the ventral surface (arrow). (D) Distribution of embryonic lethal phenotypes of *hmp-1(fe4)* and *zoo-1(RNAi);hmp-1(fe4)* animals. (E, F) Representative confocal images of F-actin staining in a *hmp-1(fe4)* (E) and *zoo-1(RNAi);hmp-1(fe4)* (F) embryo. The organization of circumferential actin filaments is consistently and markedly disrupted in *zoo-1(RNAi);hmp-1(fe4)* embryos. Scale bar, 10 μm.

Table 1

zoo-1 lethality in *rrf-3*, *hmp-1(fe4)*, and *hmp-2(qm39)*

Genotype	% Lethality	SD (n*)
rrf-3(pk1426)	11.4	±6.3 (272)
zoo-1(RNAi);rrf-3(pk1426)	33.2	±5.9 (247)
hmp-1(fe4)	77.5	±7.9 (844)
zoo-1(RNAi);hmp-1(fe4)	99.6	±1.8 (818)
zoo-1(cxTi8317);hmp-1(fe4)	99.8	±0.6 (1114)
hmp-2(qm39)	6	±1.2 (832)
zoo-1(RNAi);hmp-2(qm39)	60	±4.6 (508)

* Number of embryos counted. Numbers are the sum of at least three separate experiments for each genotype.